

Engineering mesenchymal stromal cells with neutralizing and anti-inflammatory capability against SARS-CoV-2 infection

Xiaoqing Zhang,^{1,2,4} Ping Han,^{1,2,4} Haiyong Wang,^{1,2,4} Yanqin Xu,^{1,2,4} Fanlin Li,^{1,2,4} Min Li,^{1,2,4} Lilv Fan,^{1,2} Huihui Zhang,^{1,2} Qiang Dai,^{1,2} Hao Lin,^{1,2} Xinyue Qi,^{1,2} Jie Liang,^{1,2} Xin Wang,³ and Xuanming Yang^{1,2}

¹Sheng Yushou Center of Cell Biology and Immunology, School of Life Sciences and Biotechnology, Shanghai Jiao Tong University, Shanghai 200240, China; ²Joint International Research Laboratory of Metabolic & Developmental Sciences, Shanghai Jiao Tong University, Shanghai 200240, China; ³Shanghai Longyao Biotechnology Limited, Shanghai 201203, China

The emergence of the novel human severe acute respiratory syndrome coronavirus-2 (SARS-CoV-2) has led to the pandemic of coronavirus disease 2019 (COVID-19), which has markedly affected global health and the economy. Both uncontrolled viral replication and a proinflammatory cytokine storm can cause severe tissue damage in patients with COVID-19. SARS-CoV-2 utilizes angiotensin-converting enzyme 2 (ACE2) as its entry receptor. In this study, we generated ACE2 extracellular domain-Fc and single-chain variable fragment-interleukin 6 (IL-6) single-chain variable fragment against IL-6 receptor (scFv-IL6R)-Fc fusion proteins to differentially neutralize viruses and ameliorate the cytokine storm. The human ACE2 (hACE2)₁₋₇₄₀-Fc fusion protein showed a potent inhibitory effect on pseudo-typed SARS-CoV-2 entry and a good safety profile in mice. In addition, scFv-IL6R-Fc strongly blocked IL-6 signal activation. We also established a mesenchymal stromal cell (MSC)-based hACE2₁₋₇₄₀-Fc and scFv-IL6R-Fc delivery system, which could serve as a potential therapy strategy for urgent clinical needs of patients with COVID-19.

INTRODUCTION

Severe acute respiratory syndrome coronavirus-2 (SARS-CoV-2) belongs to the genus *Betacoronavirus* and is closely related to the SARS-like coronavirus in bats. Phylogenetic analysis revealed that its genome sequence is approximately 80% similar to that of SARS-CoV. These two viruses exhibit ~74% amino acid sequence similarity at the receptor-binding domain (RBD) of the spike gene, suggestive of a possible common host receptor. Angiotensin-converting enzyme 2 (ACE2) has been recognized as a critical entry receptor for both SARS-CoV-2 and SARS-CoV.^{1,2} In comparison with the spike protein of SARS-CoV, the SARS-CoV-2 spike protein exhibits higher binding affinity to human ACE2 (hACE2); this difference may have contributed to the higher transmission rate of SARS-CoV-2,^{3,4} implying the importance of ACE2-dependent viral entry into cells. ACE2 is primarily expressed in lung alveolar epithelial type II cells, which are crucial for the gas-exchange function of the lungs.^{5,6} Severe lung injury in some patients with coronavirus disease 2019 (COVID-19) may stem from the dysfunction of these cells.⁷ ACE2 is also expressed in other organs such as the heart, liver, intestine, testis, kidney, and blood vessels,⁸⁻¹² which may explain the multiple

organ dysfunction syndrome (MODS) induced by SARS-CoV-2 infection.¹³ Apart from being the entry receptor of SARS-CoV, ACE2 facilitates tissue repair after lung injury.¹⁴

The interaction between the spike protein of SARS-CoV-2 and ACE2 is imperative for the viral entry into cells. Soluble ACE2 may act as a potential viral entry blocker by competing with membranous ACE2. Several studies have reported the antiviral effects of soluble ACE2-based therapeutics. Soluble ACE2, which removes the transmembrane domain from intact ACE2, is sufficient for neutralizing SARS-CoV-2 infection *in vitro* and *in vivo*.^{7,15} To enhance its half-life *in vivo*, soluble ACE2 was fused with an Fc fragment.^{16,17} Various approaches have been directed to enhance the affinity of soluble ACE2 toward the spike protein or the RBD of the spike protein as an attempt to improve its function as a competitive inhibitor of membranous ACE2.¹⁸⁻²⁰ In addition, mutations were introduced for the inactivation of the enzymatic activity of soluble ACE2 to avoid any adverse cardiovascular effects caused by its catalytic activity.^{19,21} *De novo* protein design and computer-based peptide design have also been applied for engineering native soluble ACE2 to generate potential SARS-CoV-2 entry blockers.²²⁻²⁴ These studies highlight the importance of ACE2-based therapeutics for treating COVID-19. However, whether cell therapy can be used for the delivery of ACE2-based therapeutics is unclear.

Cell-based therapies, including immune cell and stem cell therapies, are currently being evaluated in the clinic for a wide range of diseases such as cancer, neurodegenerative disorders, and autoimmune diseases. As a representative of cell therapy, mesenchymal stromal cell (MSC)-based therapy is most widely used in clinics, with more than 1,138 registered clinical trials until 2020.²⁵ MSCs can be obtained

Received 24 November 2020; accepted 7 May 2021;
<https://doi.org/10.1016/j.omtm.2021.05.004>

⁴These authors contributed equally

Correspondence: Xuanming Yang, Sheng Yushou Center of Cell Biology and Immunology, School of Life Sciences and Biotechnology, Shanghai Jiao Tong University, 800 Dongchuan Road, Shanghai 200240, China.

E-mail: xuanmingyang@sjtu.edu.cn



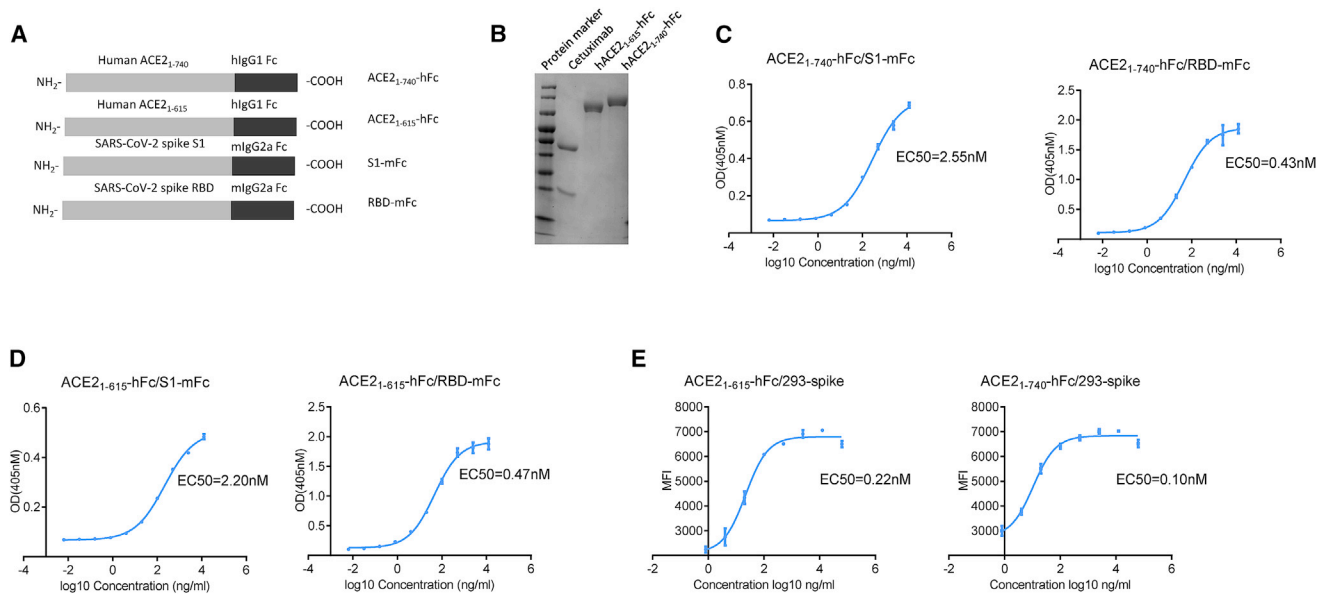


Figure 1. ACE2-Fc could bind to the SARS-CoV-2 spike protein with high affinity

(A) Schematic diagram of the ACE2 and SARS-CoV-2 spike-derived fusion protein used in this study. (B) SDS-PAGE analysis of purified indicated protein. (C and D) ELISA-binding curves of ACE2_{1–615}-hFc and ACE2_{1–740}-hFc to the immobilized S1 or RBD of the SARS-CoV-2 spike. (E) Mean fluorescence intensity (MFI) of binding of ACE2_{1–615}-hFc and ACE2_{1–740}-hFc to 293-spike cells, as determined by flow cytometry. Data represent mean \pm SD. Representative results of one from four (B) and three (C–E) repeated experiments are shown.

from different sources such as the bone marrow, cord blood, skin, Wharton's jelly, and umbilical cord tissue.²⁶ MSCs can self-renew and differentiate into adipocytes, chondrocytes, and osteocytes under specific *in vitro* culture conditions.²⁷ The multi-potent differential potential, tissue repair ability, and anti-inflammatory properties of MSCs potentiate their clinical development for the treatment of hematopoietic failure,²⁸ graft-versus-host diseases, and autoimmune diseases.^{29,30} In addition, MSCs exert paracrine functions by secreting soluble factors and releasing extracellular vesicles and possess the innate ability to transport cargos to inflammation sites, thus serving as promising drug-delivery vectors in preclinical models.³¹

Approximately 5% of patients infected with SARS-CoV-2 develop severe lung injury symptoms, accompanied with overwhelmed immune activation. Some antiviral and anti-inflammatory drugs have been tested for treating COVID-19.³² However, these single-target drugs offer limited clinical benefits. Thus, drugs targeting the virus itself and ameliorating the tissue damage are urgently warranted to treat severe COVID-19. Here, we present an MSC-based cell therapy to simultaneously block SARS-CoV-2 entry and inhibit the virus-induced cytokine storm. This dual-targeting strategy provides a rapid and translational approach for COVID-19 treatment.

RESULTS

ACE2-Fc could bind to the SARS-CoV-2 spike protein with high affinity

SARS-CoV-2 is known to enter permissive cells through ACE2;^{1,33} the competitive, soluble extracellular domain of ACE2 might poten-

tially act as a viral entry blocker. To test whether the ACE2 extracellular domain could block SARS-CoV-2 entry, we generated two recombinant ACE2-Fc fusion proteins comprising 1–615 or 1–740 amino acid residues of ACE2 fused to the human immunoglobulin G1 (IgG1) Fc (hFc) portion (Figures 1A and 1B). We then characterized their binding profiles to the SARS-CoV-2 spike protein. With the use of the same strategy, we developed two more recombinant SARS-CoV-2 spike-Fc fusion proteins carrying 1–685 (S1) or 319–541 (RBD) amino acid residues of ACE2 fused to the mouse IgG2a Fc (mFc) portion (Figure 1A). An enzyme-linked immunosorbent assay (ELISA) showed that both ACE2_{1–615}-hFc and ACE2_{1–740}-hFc bound to S1-mFc and RBD-mFc with similar affinities (Figures 1C and 1D). These data suggest that the S1 and RBD regions are essential for the binding between the ACE2 and SARS-CoV-2 spike protein. To test the binding ability of ACE2-hFc fusion protein to SARS-CoV-2 spike protein under physiological conditions, we established a 293-spike cell line that stably expressed the SARS-CoV-2 spike protein. Flow cytometry analysis showed that both ACE2_{1–615}-hFc and ACE2_{1–740}-hFc bound to the 293-spike cell line with similar affinity (Figure 1E). These data suggest that the extracellular domain of the ACE2-Fc fusion protein can bind to the SARS-CoV-2 spike protein with high affinity and could be used as a potential entry blocker.

ACE2-Fc could block the entry of pseudo-typed SARS-CoV-2 into ACE2⁺ cells

With the consideration of the potential risk of severe COVID-19 induced by SARS-CoV-2 infection, the research on SARS-CoV-2

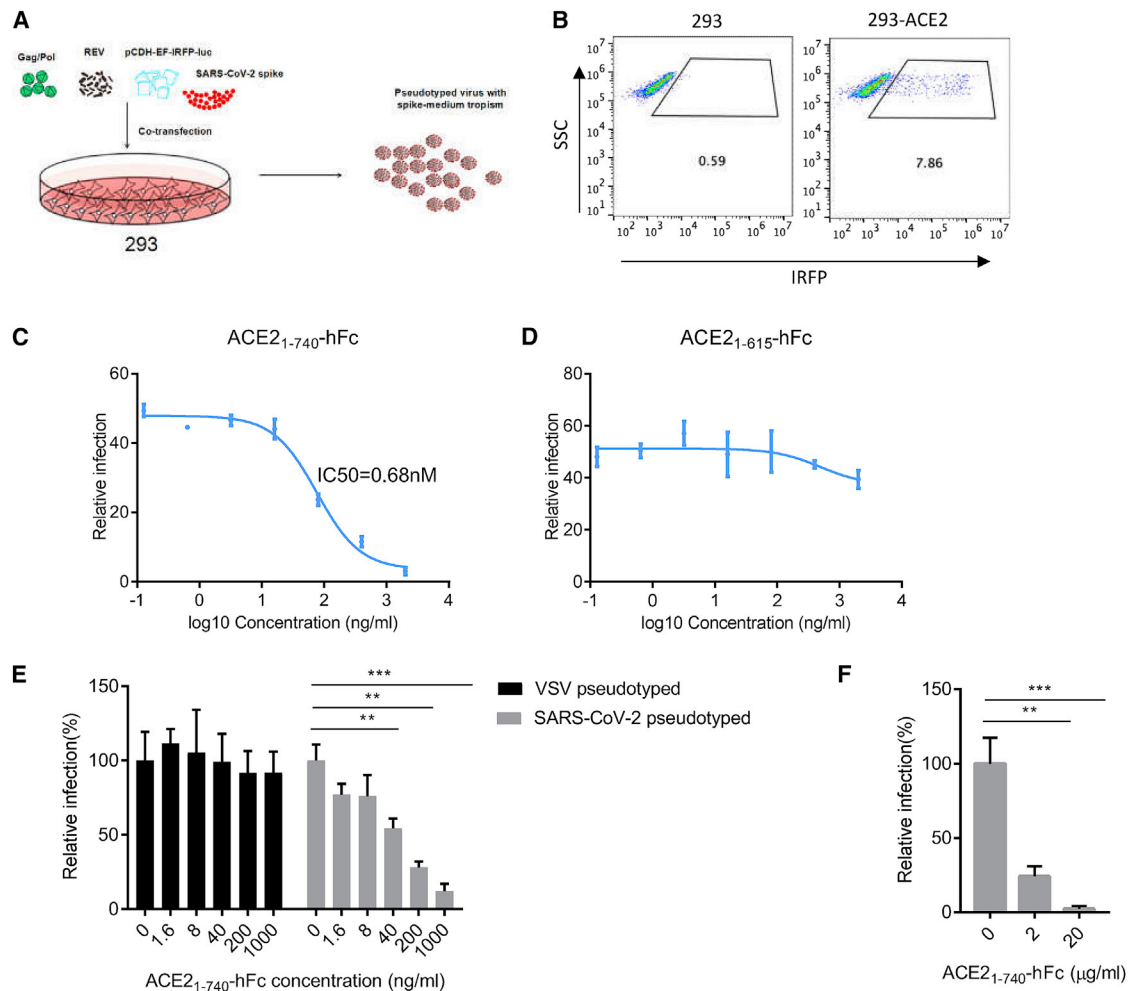


Figure 2. ACE2₁₋₇₄₀-hFc blocked the pseudo-typed SARS-CoV-2 infection

(A) Schematic diagram of pseudo-typed SARS-CoV-2 used in this study. (B) 293 or 293-ACE2 cells were infected with pseudo-typed SARS-CoV-2, and the reporter IRFP was analyzed 48 h post-infection. (C and D) Lentiviruses pseudo-typed with the SARS-CoV-2 spike protein were incubated with indicated concentrations of ACE2₁₋₆₁₅-hFc and ACE2₁₋₇₄₀-hFc for 15 min before infection. Fluorescent IRFP-positive 293-ACE2 cells were measured by flow cytometry. (E) Lentiviruses pseudo-typed with the VSV-G glycoprotein or SARS-CoV-2 spike protein were incubated with indicated concentrations of ACE2₁₋₇₄₀-hFc for 15 min before infecting 293-ACE2 cells. Fluorescent IRFP-positive cells were measured by flow cytometry. (F) Lentiviruses pseudo-typed with the SARS-CoV-2 spike protein were incubated with indicated concentrations of ACE2₁₋₆₁₅-hFc and ACE2₁₋₇₄₀-hFc for 15 min before infecting A549-ACE2 cells. Fluorescent IRFP-positive cells were measured by flow cytometry. Data represent mean \pm SD. Representative results of one from three (B–F) repeated experiments are shown. ** $p < 0.01$, *** $p < 0.001$.

must be conducted in laboratories with a biosafety level (BSL)-3 or higher. To overcome this hurdle in SARS-CoV-2 research, we established a pseudo-typed SARS-CoV-2 system by replacing vesicular stomatitis virus-G (VSV-G) with the SARS-CoV-2 spike protein to produce a pseudo-typed virus using the well-defined, third-generation lentivirus system (Figure 2A). We first checked the infection ability of this pseudo-typed virus in both ACE2⁺ and ACE2⁻ 293 cells. Pseudo-typed SARS-CoV-2 could only infect ACE2⁺ 293 cells but not ACE2⁻ 293 cells, suggestive of the SARS-CoV-2 spike, protein-mediated, ACE2-dependent entry process (Figure 2B). With the use of this pseudo-typed virus system, we tested the blocking efficacy of ACE2₁₋₆₁₅-Fc and ACE2₁₋₇₄₀-Fc. Indeed, ACE2₁₋₇₄₀-Fc could

strongly inhibit the entry of pseudo-typed SARS-CoV-2 into 293-ACE2 cells with a half-maximal inhibitory concentration (IC₅₀) of ~ 0.68 nM (Figure 2C). Surprisingly, ACE2₁₋₆₁₅-Fc had a very minor blocking effect on the entry of pseudo-typed SARS-CoV-2 despite its similar binding profile to S1-mFc, RBD-mFc, and 293-spike cells (Figures 1C–1E and 2D). To further test the specificity of the ACE2₁₋₇₄₀-hFc-mediated blockade of the pseudo-typed SARS-CoV-2, we investigated the blocking effect of ACE2₁₋₇₄₀-hFc on the entry of pseudo-typed VSV. Although ACE2₁₋₇₄₀-Fc inhibited $\sim 80\%$ pseudo-typed SARS-CoV-2 infection, it did not affect the infection by pseudo-typed VSV (Figure 2E). To determine whether the ACE2₁₋₇₄₀-Fc-mediated blockade could be applicable to other

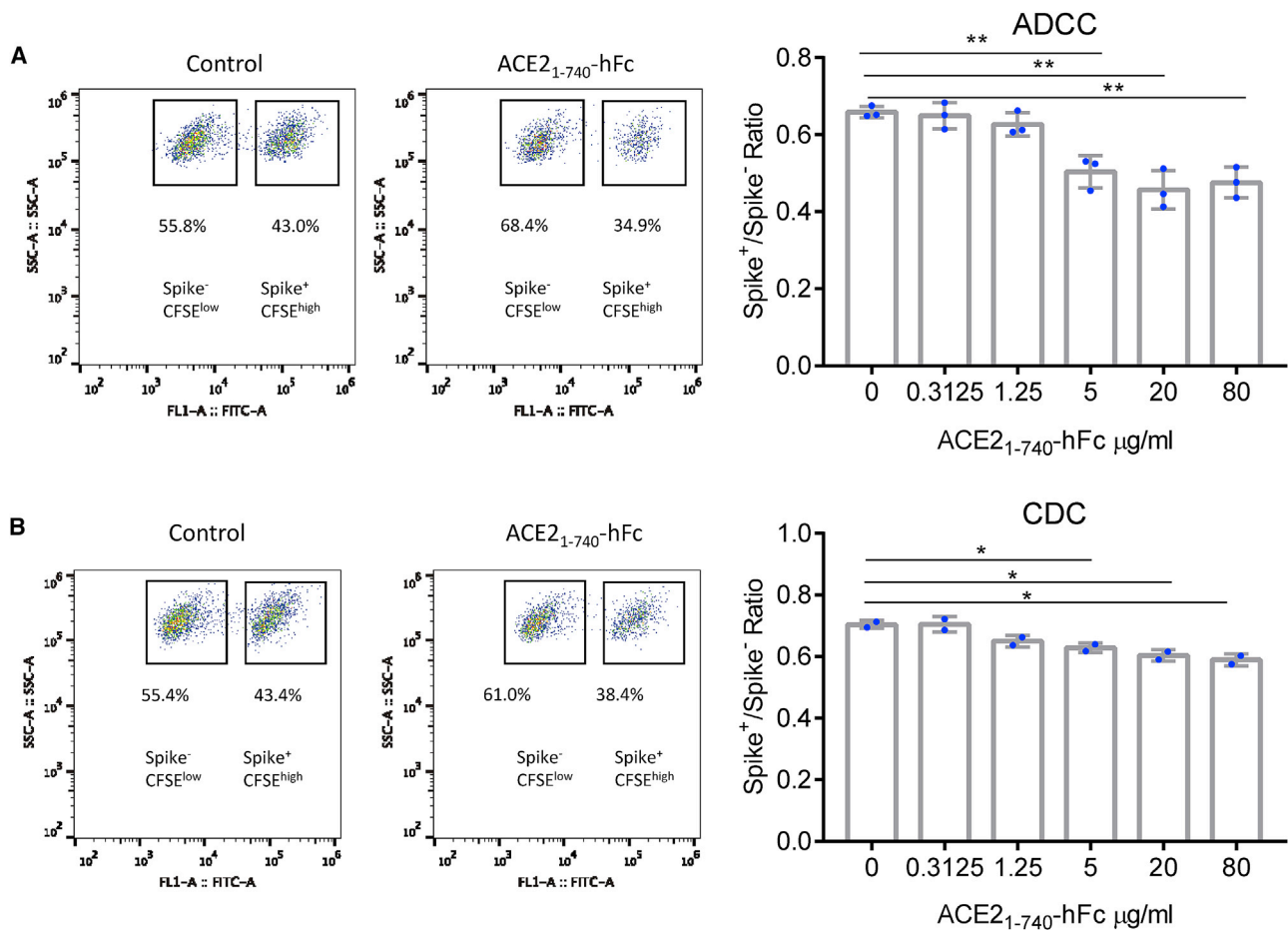


Figure 3. ACE2₁₋₇₄₀-hFc-induced death of SARS-CoV-2 spike-positive cells through ADCC and CDC

(A) Raji and Raji-spike cells were labeled with different concentrations of CFSE and co-cultured with human primary NK cells in the presence of indicated concentrations of ACE2₁₋₇₄₀-hFc. The ADCC effect was measured by flow cytometry analysis and calculated by the ratio of Raji-spike-CFSE^{high} and Raji-CFSE^{low}. (B) Raji and Raji-spike cells were labeled with different concentrations of CFSE, co-cultured, and supplemented with human AB serum in the presence of indicated concentrations of ACE2₁₋₇₄₀-hFc. The CDC effect was measured by flow cytometry analysis and calculated from the ratio of Raji-spike-CFSE^{high} and Raji-CFSE^{low}. Data represent mean ± SD. Representative results of one from three (A and B) repeated experiments are shown. *p < 0.05, **p < 0.01.

cell types, we performed a similar assay on the lung epithelial A549-ACE2 cell line. Consistent with the data from 293-ACE2 cells, ACE2₁₋₇₄₀-Fc significantly blocked the entry of pseudo-typed SARS-CoV-2 into A549-ACE2 cells (Figure 2F). Therefore, ACE2₁₋₇₄₀-hFc blocked the pseudo-typed SARS-CoV-2 infection by competing with the membrane-anchored entry receptors.

ACE2-Fc-mediated cytotoxicity against SARS-CoV-2 spike-positive cells is directed through the Fc portion

There are two functional portions of the ACE2₁₋₇₄₀-hFc fusion protein. The extracellular domain, ACE2₁₋₇₄₀, functions as a competitive binding factor to the membrane-anchored SARS-CoV-2 receptor ACE2, and the Fc portion mediates multiple functions by engaging Fc gamma receptor (FcγR)-positive cells and complements.³⁴ To verify whether ACE2₁₋₇₄₀-hFc could induce death of SARS-CoV-2 spike-positive cells through antibody-dependent cell-mediated cytotoxicity

(ADCC), we performed a natural killer (NK) cell and Raji-spike cell co-culture assay in the presence of ACE2₁₋₇₄₀-hFc. Given the high binding affinity of IgG1 to active FcγRs,³⁵ ACE2₁₋₇₄₀-hFc induced significant ADCC and lysed more Raji-spike cells than Raji cells (Figure 3A). This observation highlights the potential lysis effect on virus-infected cells *in vivo*. We also tested whether ACE2₁₋₇₄₀-hFc could induce complement-dependent cytotoxicity (CDC). In the presence of complements, ACE2₁₋₇₄₀-hFc induced more lysis of spike-positive cells than that of spike-negative cells (Figure 3B). Taken together, ACE2₁₋₇₄₀-hFc could potentially eliminate virus-infected, spike-positive cells through both ADCC and CDC.

Safety profile of ACE2₁₋₇₄₀-hFc *in vivo*

ACE2 is a carboxypeptidase that potently degrades angiotensin II to angiotensin 1-7.³⁶ ACE2 antagonizes the activation of the classical renin-angiotensin (RAS) system and protects against organ damage,

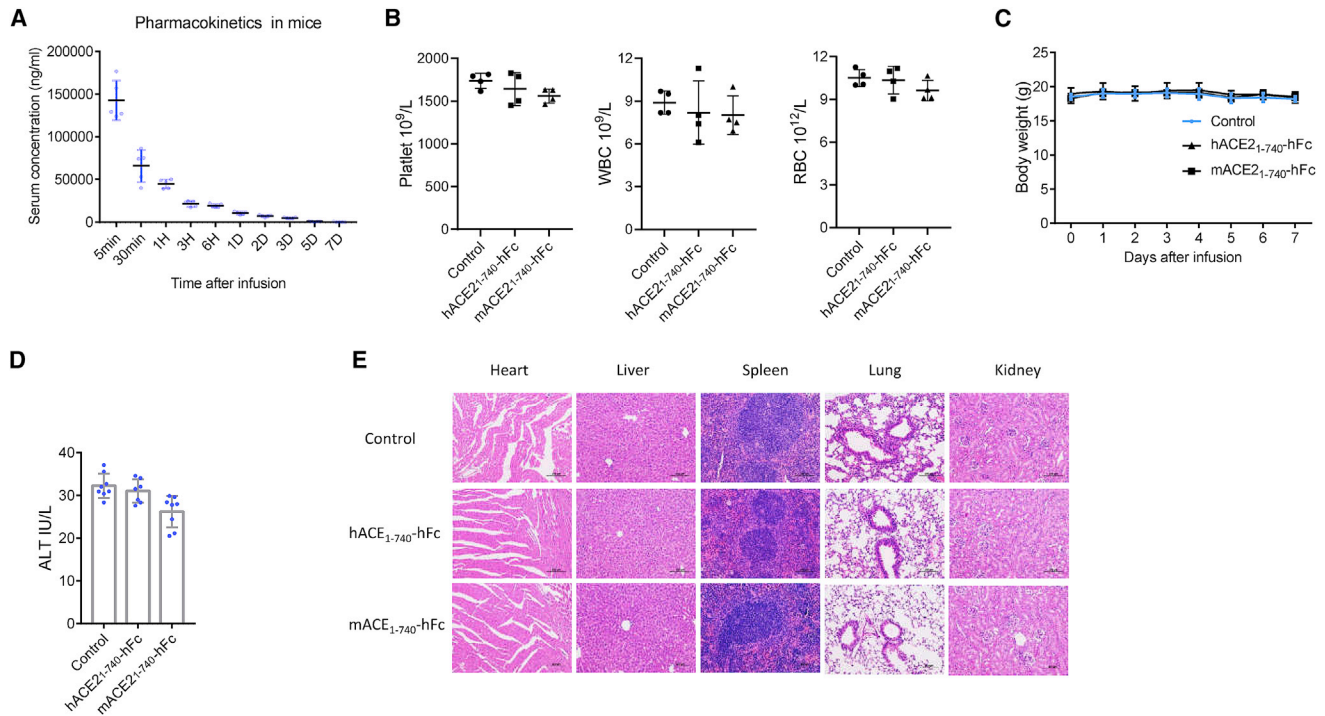


Figure 4. Safety profile of ACE2₁₋₇₄₀-hFc in mice

(A) C57BL/6 mice received a single injection of 100 μ g ACE2₁₋₇₄₀-hFc. The serum concentration was determined by ELISA at indicated time points. (B–E) C57BL/6 mice received a single injection of 100 μ g ACE2₁₋₇₄₀-hFc. 7 days later, the hematology, body weight, and hematoxylin and eosin (H&E) staining of indicated organs were analyzed. Data represent mean \pm SEM. Representative results of one from two (A–E) repeated experiments are shown.

hypertension, diabetes, and cardiovascular diseases.³⁷ Whether exogenous exposure to ACE2₁₋₇₄₀-hFc affects the normal physiological status is, however, unclear. First, we tested the *in vivo* half-life of hACE2₁₋₇₄₀-hFc in mice and found it to be approximately 8.22 h (Figure 4A). We subsequently collected different tissues and investigated the potential effect of ACE2₁₋₇₄₀-hFc on tissue damage. There were no differences in hematological features, body weight change, alanine aminotransferase (ALT), and immune cell infiltration in organs such as the heart, liver, spleen, lung, and kidney (Figures 4B–4E). Although the enzyme activity of hACE2₁₋₇₄₀-hFc is well reported in mice,³⁸ two potential factors may affect the evaluation of side effects, namely, the potential immune response against human protein hACE2 in mice and different interaction networks of hACE2 and mouse ACE2 (mACE2). To avoid these limitations, we performed similar experiments using mACE2₁₋₇₄₀-hFc and observed no adverse effects 7 days after treatment (Figures 4B–4E). Taken together, ACE2₁₋₇₄₀-hFc was well tolerated in mice without any obvious side effects.

Engineered MSCs can be a potential drug-development strategy for COVID-19 treatment

The clinical translation of protein-based therapeutics can be time consuming owing to good manufacturing practices (GMP) production and quality control, which may not be feasible for the urgent need for treating COVID-19. Therefore, other drug-delivery systems

should be considered to save time. MSCs have been widely used for treating autoimmune diseases and as vectors for protein drug delivery. We generated an MSC cell line stably expressing ACE2₁₋₇₄₀-hFc (MSC-ACE2₁₋₇₄₀-hFc) by lentiviral infection. As expected, this cell line persistently secreted ACE2₁₋₇₄₀-hFc into the culture supernatant (Figures 5A and S1). The concentration of ACE2₁₋₇₄₀-hFc in the supernatant was about 190 ng/mL after a 4-day culture. To determine whether ACE2₁₋₇₄₀-hFc in MSC-derived supernatant is bio-reactive, we first measured its ability to react with spike-positive 293 cells (Figure 5B). The MSC-secreted ACE2₁₋₇₄₀-hFc showed a binding strength similar to that of purified ACE2₁₋₇₄₀-hFc (Figure 5C). We next investigated whether ACE2₁₋₇₄₀-hFc from the MSC-derived supernatant could block pseudo-typed virus entry. Indeed, the MSC-derived supernatant showed a significant blockade effect on the entry of pseudo-typed SARS-CoV-2 into 293-ACE2 cells (Figure 5D). To test the possibility of using MSC-ACE2₁₋₇₄₀-hFc as a live drug *in vivo*, we injected these engineered MSCs into mice. The expression of ACE2-Fc in the serum lasted for more than 14 days after a single dose (Figure 5E). Further, we evaluated the bio-distribution of these MSCs, which were preferentially located in the lungs after 24 h of injection (Figure 5E). Thus, these MSCs are suitable for treating SARS-CoV-2-induced pneumonia. Therefore, the MSC-based ACE2₁₋₇₄₀-Fc delivery strategy provides a time-saving option for clinical treatment of SARS-CoV-2-induced disease.

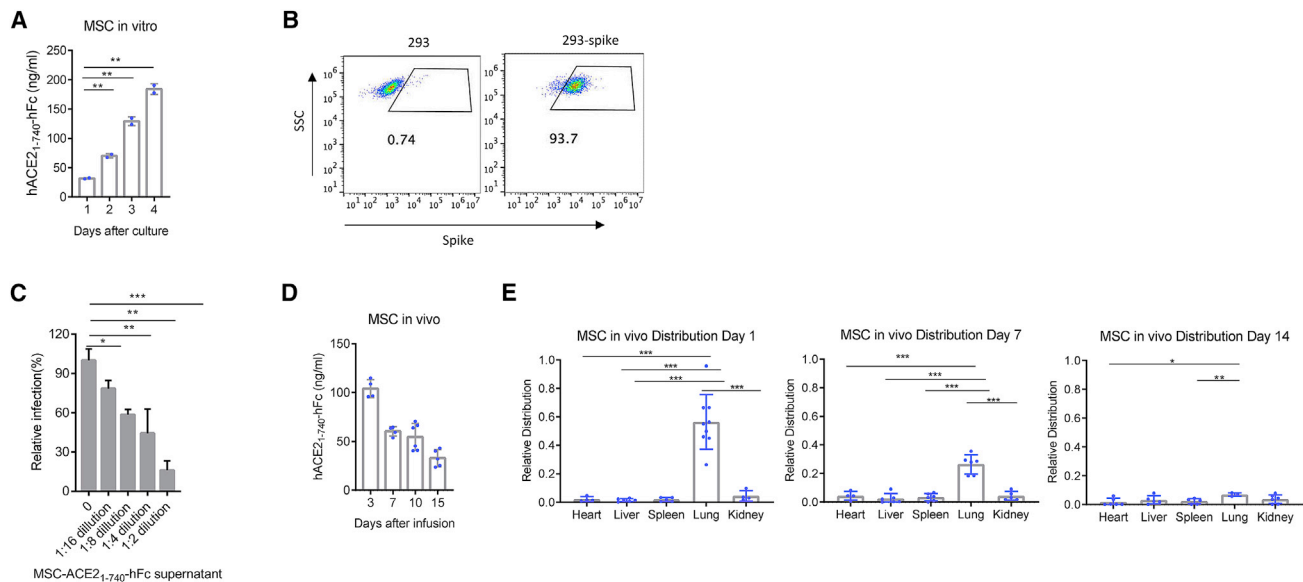


Figure 5. Characterization of ACE2₁₋₇₄₀-hFc-expressing MSCs

(A) The continuous ACE2₁₋₇₄₀-hFc production by stably engineered MSC-ACE2₁₋₇₄₀-hFc was measured by ELISA after a 1 month of culture. (B) Flow cytometry analysis of the supernatant from 293 or 293-spike cells treated with MSC-ACE2₁₋₇₄₀-hFc. (C) Lentiviruses pseudo-typed with SARS-CoV-2 spike protein were incubated with indicated dilutions of MSC-ACE2₁₋₇₄₀-hFc supernatant for 15 min before infecting 293-ACE2 cells. Fluorescent IRFP-positive cells were measured by flow cytometry. (D) MSC-ACE2₁₋₇₄₀-hFc was intravenously injected into M-NSG mice, and ACE2₁₋₇₄₀-hFc production in the serum was determined by ELISA at indicated time points. (E) MSC-ACE2₁₋₇₄₀-hFc cells were intravenously injected into M-NSG mice, and their bio-distribution in the indicated tissues was analyzed by qPCR. Data represent mean \pm SEM. Representative results of one from three (A and C) and four (B) repeated experiments are shown. Pooled results from three independent experiments are shown (D and E). * $p < 0.05$, ** $p < 0.01$, *** $p < 0.001$.

MSCs expressing variable fragment-interleukin 6 (IL-6) single-chain variable fragment against IL-6 receptor (scFv-IL6R)-Fc can potentially inhibit SARS-CoV-2-induced immune damage

The proinflammatory cytokine storm can cause tissue damage in multiple disease models. Suppression of proinflammatory cytokines such as IL-6 has been shown to mediate therapeutic effects in autoimmune diseases and the chimeric antigen receptor (CAR)-T cell-induced cytokine storm.^{39,40} For instance, tocilizumab has been used to treat COVID-19 and improve patient outcome.^{41,42} With the consideration that MSCs are capable of rapidly producing proteins and preferentially migrating to inflammatory tissues, we aimed to generate MSCs expressing single-chain variable fragment against IL-6 receptor (scFv-IL6R)-Fc to suppress the SARS-CoV-2-induced cytokine storm. We first generated and purified scFv-IL6R-Fc protein and compared its activity with that of tocilizumab. scFv-IL6R-Fc showed a similar blockade effect on the IL-6-induced TF-1 cell proliferation compared with tocilizumab (Figure 6A). We then established an MSC cell line stably expressing scFv-IL6R-Fc. After 1 month of culture, this cell line was still capable of secreting scFv-IL6R-Fc. The concentration of scFv-IL6R-Fc in the supernatant was about 300 ng/mL after a 4-day culture (Figure 6B). To test the *in vivo* performance of the MSC-derived scFv-IL6R-Fc, we injected them intravenously into mice. Interestingly, the expression of scFv-IL6R-Fc in the serum lasted for more than 14 days after administration of a single dose (Figure 6C). Therefore, scFv-IL6R-Fc-expressing MSCs can be potentially used for blocking the SARS-CoV-2-induced cytokine storm and can be com-

bined with virus-neutralizing MSC-ACE2₁₋₇₄₀-Fc to provide multi-layer protection against SARS-CoV-2 infection.

DISCUSSION

The current COVID-19 pandemic has created a greater social and economic stir than its predecessors, SARS outbreak and Middle East Respiratory Syndrome (MERS) epidemic. Although some vaccines and neutralizing antibodies have been approved for clinical usage,⁴³⁻⁵⁰ their efficacy may be compromised by the frequent viral mutations.^{51,52} Therefore, safe and effective treatments for COVID-19 are urgently warranted. SARS-CoV-2 enters permissive cells mainly through ACE2.¹ Neutralizing antibodies against the SARS-CoV-2 spike protein and soluble ACE2 receptors are potential drug candidates that can block the viral entry into cells.^{7,16} The acceptable stability, specificity, and manufacturing process have deemed neutralizing antibodies as promising candidates for drug development. Theoretically, these antibodies only affect the virus or virus-infected cells and thus, pose limited side effects *in vivo*. However, the high mutation rate may lead to the escape of the virus from neutralizing antibodies even after a single mutation. This hypothesis is supported by the observation that neutralizing antibodies against SARS-CoV have limited blocking effect on SARS-CoV-2 despite the high similarity in their RBD structures. This limitation can be avoided with a soluble ACE2-based neutralization strategy, as mutant viruses escaping soluble ACE2 will also lose the ability to infect ACE2-positive cells. One shortcoming with both

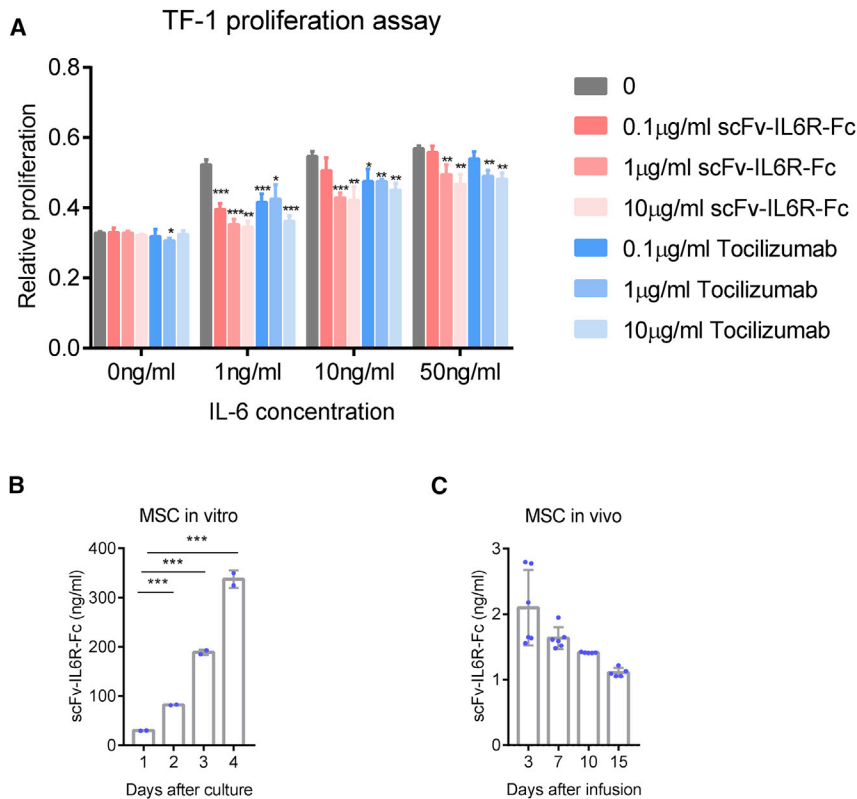


Figure 6. Characterization of scFv-IL6R-hFc-expressing MSCs

(A) Approximately 1×10^4 TF-1 cells were stimulated with IL-6 in the presence of indicated concentrations of scFv-IL6R-Fc and tocilizumab. Cell proliferation was determined 48 h later by CCK-8 assay. (B) The continuous scFv-IL6R-Fc production from stably engineered MSC-scFv-IL6R-Fc was measured by ELISA after 1 month of culture. (C) MSC-scFv-IL6R-Fc cells were intravenously injected into M-NSG mice, and the scFv-IL6R-Fc level in the serum was determined by ELISA at indicated time points. Data represent mean \pm SEM. Representative results of one from three (A and B) repeated experiments are shown. Pooled results from three independent experiments are shown (C). * $p < 0.05$, ** $p < 0.01$, *** $p < 0.001$.

neutralizing antibodies and ACE2-Fc fusion protein is the antibody-dependent enhancement effect on virus infection. Further experiments are imperative to clarify these concerns. With the consideration of the biosafety issue, our study was performed using pseudo-typed viruses. Although the entry step of pseudo-typed viruses is similar to that of live viruses, further investigation with live virus and animal models will provide more information on the efficacy of ACE2-Fc-based therapy.

ACE2 is a carboxypeptidase that potently degrades angiotensin II to angiotensin 1–7.³⁶ It plays a central role in the homeostatic control of cardiorenal action. ACE2 is a membrane protein, and its distribution is determined by the expressing cells. Soluble ACE2 is delivered to all possible tissues through the circulatory system, thereby raising the concern regarding its side effects on the cardiorenal system. Our preliminary mouse data showed no obvious side effects induced by ACE2-Fc treatment. Further investigation on the long-term side effects of ACE2 is needed in animal models before translation into clinical studies. Despite this limitation, there is one potential advantage of soluble ACE2 as a promising therapy. ACE2 has been reported to play a protective role in lung injury.¹⁴ SARS-CoV-2 infection leads to internalization of the ACE2 receptor, which may reduce ACE2 enzymatic activity and its subsequent protective effect on lung injury. Supplementation with soluble ACE2 may provide additional tissue repair effects beyond viral neutralization.

Given the important role of ACE2 in SARS-CoV-2 entry, multiple research groups have reported the applicability of soluble ACE2 as an effective entry blocker.^{16,53} In addition to using wild-type intact soluble ACE2, high-affinity ACE2 mutant,^{18,20,54} enzymatic dead mutation,^{23,55} or peptide inhibitors derived from ACE2^{56,57} provide highly promising effects for blocking SARS-CoV-2 entry. Our data indicate that the Fc portion of ACE2_{1–740}-Fc can mediate weak ADCC and CDC to eliminate virus-infected, spike-expressing cells^{58,59} and may provide additional immune-regulatory functions for improving antiviral effects. We used MSC as a drug-delivery vector; its inflammation tissue tropism may provide an advantage of targeting the drug specifically to the virus-infected tissue. Furthermore, MSCs were engineered to secrete scFv-IL6R, which could sufficiently block the IL-6 signaling pathway and prevent the overwhelming inflammation in COVID-19.

To meet the urgent need for treating SARS-CoV-2-induced COVID-19, we have developed an MSC-based cell therapy strategy. MSCs have been widely used for treating autoimmune diseases for more than 20 years.⁶⁰ There are ongoing clinical trials to evaluate the efficacy of MSCs for COVID-19 treatment, given their innate anti-inflammatory and tissue-repair activities. Here, we armed MSCs with virus neutralization and anti-cytokine storm capabilities to significantly boost their therapeutic effects. MSCs are preferentially located in inflammatory tissues, thus aiding in the targeted delivery of ACE2 fusion protein to SARS-CoV-2-infected tissues. This phenomenon significantly enhances the drug concentration in the targeted tissue and lowers the potential side effects. However, a plausible disadvantage of MSC-based therapy includes the challenges in regulating the dosage of soluble ACE2 secreted from cells. Further engineering of MSCs with on-off switchable promoters or suicide genes may provide a possible solution to overcome these hurdles.

The MSC delivery method is critical for the successful clinical treatment of COVID-19 and determines treatment efficacy and safety.

Previous studies have shown that the *in vivo* persistence of MSCs is limited,^{61–63} which restricts their potency as a delivery vector. Further optimization to reduce immunogenicity and enhance survival of MSCs *in vivo* is critical to improve their efficacy. With the consideration of the safety profile of intravenously infused MSCs, some severe COVID-19 patients are in a hypercoagulable-procoagulant state and are at high risk of thrombosis and embolization.⁶⁴ Some non-bone marrow-derived MSCs express high levels of the procoagulant tissue factor, which might induce severe thrombosis and embolization when intravenously infused in patients with COVID-19.^{64–66} Pre-screening for the expression of the procoagulant tissue factor of MSCs and the hemocompatibility test before infusion is critical for preventing this adverse effect.

The limitations of our study include the lack of the use of the SARS-CoV-2 virus and immune-competent animal models. Although pseudo-viruses are widely used to dissect the viral-entry mechanism, they are not capable of replication in host cells; this may cause overestimation of the viral-entry blockade effect of ACE2_{1–740}-Fc. Furthermore, the deficiency of non-obese diabetic (NOD)-*Prkdcsevere* combined immunodeficiency (*scid*)*Il2g^{tm1Wjl}* (NSG) mice in adaptive immune cell components may be favorable for MSC persistence *in vivo*. When allogeneic MSCs are used in the clinic, their clearance by the recipient's adaptive immune response reduces both the delivered drug concentration and its half-life. Further optimization of the *in vivo* persistence of MSCs and improvement of transgene expression will be critical before their clinical application. Owing to the lack of BSL-3 laboratory conditions, we did not evaluate the side effects of ACE2_{1–740}-Fc in virus-infected hosts. As ACE2_{1–740}-Fc showed cytotoxicity against spike-expressing cells, it may cause tissue damage upon virus infection. This should be further investigated using appropriate virus-infected models. It would also be interesting to test whether ACE2_{1–740}-Fc is effective against the mutated SARS-CoV-2 strain.

Taken together, our data indicate that ACE2-Fc can serve as a potential therapeutic agent for COVID-19 treatment with a relatively good safety profile. MSC-based viral blockade and inflammation control can provide a rapid alternative for multi-layer protection against SARS-CoV-2 infection.

MATERIALS AND METHODS

Mice

C57BL/6J mice were purchased from Beijing Vital River Laboratory Animal Technology (Beijing, China). NSG equivalent M-NSG mice were obtained from the Shanghai Model Organisms Center (Shanghai, China). All mice were maintained under specific pathogen-free conditions. Animal care and use were in accordance with institutional and NIH protocols and guidelines, and all studies were approved by the Animal Care and Use Committee of Shanghai Jiao Tong University.

Cell lines and reagents

Lenti-X 293 cells were purchased from Clontech. A549 cells were obtained from the American Type Culture Collection. Raji cells were

kindly provided by the Stem Cell Bank, Chinese Academy of Sciences (Shanghai, China). TF-1 cells were kindly provided by the Cell Resource Center, Peking Union Medical College (Beijing, China). Human NK cells and MSCs were kindly provided by Shanghai Longyao Biotechnology (Shanghai, China). Plasmids encoding the SARS-CoV-2 spike protein and ACE2 were obtained from Molecular Cloud (Nanjing, China) and sub-cloned into a pCDH-EF (System Biosciences) lentiviral vector plasmid with a puromycin-resistance marker. To establish SARS-CoV-2 spike- or ACE2-expressing cell lines, Lenti-X 293, A549, or Raji cells were infected with a SARS-CoV-2 spike- or ACE2-expressing lentivirus. After selection with puromycin, the pooled resistant cells were identified by flow cytometry. The cell culture medium was supplemented with 10% heat-inactivated fetal bovine serum (FBS), 2 mM L-glutamine, 100 units/mL penicillin, and 100 µg/mL streptomycin. Lenti-X 293 as well as A549 cells and their derivatives were cultured in complete Dulbecco's modified Eagle's medium (DMEM). Raji cells and their derivatives were cultured in complete Roswell Park Memorial Institute (RPMI) medium. Human AB serum was purchased from Gemini Bio-products (West Sacramento, CA, USA).

Production of ACE2 and spike fusion protein

For hACE2_{1–740}-hFc, hACE2_{1–615}-hFc, mACE2_{1–740}-hFc, S1-mFc, and RBD-mFc fusion protein production, DNA sequences encoding the indicated proteins (Figure S1) were cloned into the pCDH-EF vector (System Biosciences, Mountain View, CA, USA). Briefly, plasmids containing the indicated fusion protein were transiently transfected into Lenti-X 293 cells using polyethylenimine. From days 1 to 5 after transfection, the medium was refreshed with DMEM supplemented with 1% FBS. All supernatants containing the recombinant proteins were collected and pooled. Purification was carried out using a Diamond Protein A column according to the manufacturer's protocol (Bestchrom, Shanghai, China).

Neutralization assay with pseudo-typed SARS-CoV-2

Lenti-X 293 cells were transfected with lentivirus package component plasmids, Gap/pol (Addgene; #12251), RSV-Rev (Addgene; #12253), pCDH-EF-infrared-fluorescent protein (IRFP)-luciferase (luc), and pcDNA3.1(+)-2019-nCoV-spike-P2A-EGFP (Molecular Cloud; #MC_0101087). Supernatants containing lentivirus particles were collected 48 and 72 h post-transfection by ultracentrifugation for direct usage or concentration. The viral titer (transduction units per milliliter) was determined by flow cytometry analysis of transduced Lenti-X 293-ACE2 cells. In the viral neutralization assay, hACE2_{1–740}-hFc and hACE2_{1–615}-hFc were serially diluted to indicated concentrations in complete DMEM. Diluted hACE2_{1–740}-hFc and hACE2_{1–615}-hFc were incubated with pseudo-typed lentiviral particles for 15 min at room temperature (20°C~25°C), inoculated on 293-ACE2 or A549-ACE2 monolayers in 96-well plates in the presence of 10 µg/mL polybrene, and further incubated at 37°C for 48 h. For A549-ACE2 infection, the samples were subjected to 60 min spinning at 1,258 × g at 32°C to improve the infection efficiency. Near-IRFP reporter activity was measured using Cytotoflex S (Beckman Coulter). The percentage of infectivity was calculated as

the ratio of IRFP readout in the presence of fusion protein normalized to that in the absence of fusion protein. The IC_{50} value was determined using a four-parameter logistic regression model (GraphPad Prism version 8).

ELISA and flow cytometry analysis of hACE2₁₋₇₄₀-hFc and hACE2₁₋₆₁₅-hFc

ELISA plates (Jet Biofil, Guangzhou, China) were coated with 2 μ g/mL of RBD-mFc at 4°C for overnight. Plates were washed thrice with phosphate-buffered saline (PBS) containing 0.05% Tween 20 and blocked with 2% FBS in PBS at room temperature for 1 h. Samples with diluted, hACE2₁₋₇₄₀-hFc and hACE2₁₋₆₁₅-hFc were added to the wells, and the plates were incubated for 1 h at room temperature. Plates were then washed thrice and incubated with an alkaline phosphatase (AP)-conjugated goat anti-hFc secondary antibody (Jackson ImmunoResearch) diluted 1:2,000 in a blocking buffer for 1 h at room temperature. AP activity was measured at 405 nm using p-nitrophenyl phosphate (Guangzhou Howei Pharmaceutical Technology, Guangzhou, China) on an ELISA plate reader (Molecular Devices). The half-maximum effective concentration (EC_{50}) binding values were calculated using GraphPad Prism (version 8).

293-spike cells were incubated with indicated samples containing ACE2₁₋₇₄₀-hFc or ACE2₁₋₆₁₅-hFc at 4°C for 30 min, washed thrice with 2% FBS in PBS, and incubated with 1:200 diluted Alexa Fluor 647-conjugated goat anti-hFc antibodies (Jackson ImmunoResearch). Samples were analyzed on a Cytoflex S (Beckman Coulter), and data were analyzed using FlowJo software (Tree Star).

Lentivirus production

Lentivirus was produced by transient transfection of Lenti-X 293 with a four-plasmid system. Supernatants containing lentivirus particles were collected 48 and 72 h post-transfection and used to establish stable cell lines.

In vitro ADCC and CDC assays

Raji and Raji-spike cells were labeled with 5 or 50 μ M carboxyfluorescein succinimidyl amino ester (CFSE), respectively, according to the manufacturer's protocol (MedChemExpress, Shanghai, China). Approximately 2×10^4 CFSE-labeled Raji and Raji-spike cells were co-cultured with 4×10^5 primary NK cells or supplemented with 10% human AB serum in the presence of various concentrations of hACE2₁₋₇₄₀-hFc. After 48 h, the cells were analyzed by flow cytometry. The ratio of CFSE^{high}/CFSE^{low} was used to indicate the relative death of Raji-spike cells versus Raji cells.

In vivo characterization of hACE2₁₋₇₄₀-hFc

Pharmacokinetics were determined in C57BL/6 mice after a single injection of 100 μ g ACE2₁₋₇₄₀-hFc. Serum concentrations at indicated time points were determined by ELISA using immobilized RBD-mFc. C57BL/6 mice received a single injection of 100 μ g of ACE2₁₋₇₄₀-hFc. 7 days later, hematology, body weight, and hematoxylin and eosin (H&E) staining of the indicated organs were analyzed. H&E staining was performed by Servicebio (Wuhan, China).

Bio-distribution of MSC-ACE2-Fc

M-NSG mice were intravenously injected with $5-7.5 \times 10^5$ MSC-ACE2-Fc through retro-orbital sinus. On days 1, 7, and 14 after injection, the heart, liver, spleen, lung, and kidney were collected. Genomic DNA was isolated from these organs using an E.Z.N.A. Tissue DNA Kit I (Omega Bio-tek). The relative distribution of human MSCs was quantified by real-time polymerase chain reaction (PCR) using primers (5'-aagtcataagtcggttgaggaggagat-3' and 5'-cca-gattctgcagtttagcatctgtgt-3') against the human *IL2RG* gene, which was absent in M-NSG mice.

TF-1 proliferation assay

TF-1 cells were seeded in flat-bottomed, 96-well plates at 10,000 cells/well in the presence of 1, 10, or 50 ng/mL IL-6 (Sino Biological, Beijing, China). The cells were then incubated with 0.1, 1, or 10 μ g/mL of scFv-IL6R-Fc or tocilizumab (Roche) for 48 h. Following incubation, cell proliferation was measured by the Cell Counting Kit (CCK)-8 assay (Dojindo Molecular Technologies, Shanghai, China) according to the manufacturer's protocol.

Statistical analysis

Data are expressed as mean \pm standard deviation (SD) or standard error of the mean (SEM). The data of two groups were compared using a two-tailed unpaired Student's t test. Statistically significant differences are indicated by * $p < 0.05$, ** $p < 0.01$, and *** $p < 0.001$.

SUPPLEMENTAL INFORMATION

Supplemental information can be found online at <https://doi.org/10.1016/j.omtm.2021.05.004>.

ACKNOWLEDGMENTS

All relevant data are available from the authors upon request. Supporting data for this study are available from the corresponding author upon reasonable request. X.Y. was supported by the National Natural Science Foundation of China (81971467 and 81671643), National Key Research and Development Program of China (2016YFC1303400), Sheng Yushou Foundation, and Shanghai Jiao Tong University Scientific and Technological Innovation Funds. P.H. was supported by the National Natural Science Foundation of China (81901689).

AUTHOR CONTRIBUTIONS

X.Y. designed the project. X.Z., P.H., H.W., Y.X., M.L., F.L., H.Z., Q.D., H.L., X.Q., J.L., X.W., and X.Y. performed the experiments. X.Z. and X.Y. analyzed the results and wrote the manuscript.

DECLARATION OF INTERESTS

The authors declare no competing interests.

REFERENCES

- Zhou, P., Yang, X.L., Wang, X.G., Hu, B., Zhang, L., Zhang, W., Si, H.R., Zhu, Y., Li, B., Huang, C.L., et al. (2020). A pneumonia outbreak associated with a new coronavirus of probable bat origin. *Nature* 579, 270–273.

2. Li, W., Moore, M.J., Vasilieva, N., Sui, J., Wong, S.K., Berne, M.A., Somasundaran, M., Sullivan, J.L., Luzuriaga, K., Greenough, T.C., et al. (2003). Angiotensin-converting enzyme 2 is a functional receptor for the SARS coronavirus. *Nature* *426*, 450–454.
3. Wang, Q., Zhang, Y., Wu, L., Niu, S., Song, C., Zhang, Z., Lu, G., Qiao, C., Hu, Y., Yuen, K.Y., et al. (2020). Structural and Functional Basis of SARS-CoV-2 Entry by Using Human ACE2. *Cell* *181*, 894–904.e9.
4. Wrapp, D., Wang, N., Corbett, K.S., Goldsmith, J.A., Hsieh, C.-L., Abiona, O., Graham, B.S., and McLellan, J.S. (2020). Cryo-EM structure of the 2019-nCoV spike in the prefusion conformation. *Science* *367*, 1260–1263.
5. Zhao, Y., Zhao, Z., Wang, Y., Zhou, Y., Ma, Y., and Zuo, W. (2020). Single-cell RNA expression profiling of ACE2, the putative receptor of Wuhan 2019-nCoV. *bioRxiv*. <https://doi.org/10.1101/2020.01.26.919985>.
6. Dobbs, L.G. (1989). Pulmonary surfactant. *Annu. Rev. Med.* *40*, 431–446.
7. Monteil, V., Kwon, H., Prado, P., Hagelkrüys, A., Wimmer, R.A., Stahl, M., Leopoldi, A., Garreta, E., Hurtado Del Pozo, C., Prosper, F., et al. (2020). Inhibition of SARS-CoV-2 Infections in Engineered Human Tissues Using Clinical-Grade Soluble Human ACE2. *Cell* *181*, 905–913.e7.
8. Crackower, M.A., Sarao, R., Oudit, G.Y., Yagil, C., Kozieradzki, I., Scanga, S.E., Oliveira-dos-Santos, A.J., da Costa, J., Zhang, L., Pei, Y., et al. (2002). Angiotensin-converting enzyme 2 is an essential regulator of heart function. *Nature* *417*, 822–828.
9. Danilczyk, U., and Penninger, J.M. (2006). Angiotensin-converting enzyme II in the heart and the kidney. *Circ. Res.* *98*, 463–471.
10. Guan, W.J., Ni, Z.Y., Hu, Y., Liang, W.H., Ou, C.Q., He, J.X., Liu, L., Shan, H., Lei, C.L., Hui, D.S.C., et al.; China Medical Treatment Expert Group for Covid-19 (2020). Clinical Characteristics of Coronavirus Disease 2019 in China. *N. Engl. J. Med.* *382*, 1708–1720.
11. Gu, J., Gong, E., Zhang, B., Zheng, J., Gao, Z., Zhong, Y., Zou, W., Zhan, J., Wang, S., Xie, Z., et al. (2005). Multiple organ infection and the pathogenesis of SARS. *J. Exp. Med.* *202*, 415–424.
12. Hamming, I., Timens, W., Bulthuis, M.L., Lely, A.T., Navis, G., and van Goor, H. (2004). Tissue distribution of ACE2 protein, the functional receptor for SARS coronavirus. A first step in understanding SARS pathogenesis. *J. Pathol.* *203*, 631–637.
13. Huang, C., Wang, Y., Li, X., Ren, L., Zhao, J., Hu, Y., Zhang, L., Fan, G., Xu, J., Gu, X., et al. (2020). Clinical features of patients infected with 2019 novel coronavirus in Wuhan, China. *Lancet* *395*, 497–506.
14. Zhang, H., Penninger, J.M., Li, Y., Zhong, N., and Slutsky, A.S. (2020). Angiotensin-converting enzyme 2 (ACE2) as a SARS-CoV-2 receptor: molecular mechanisms and potential therapeutic target. *Intensive Care Med.* *46*, 586–590.
15. Zoufaly, A., Poglitsch, M., Aberle, J.H., Hoepfer, W., Seitz, T., Traugott, M., Grieb, A., Pawelka, E., Laferl, H., Wenisch, C., et al. (2020). Human recombinant soluble ACE2 in severe COVID-19. *Lancet Respir. Med.* *8*, 1154–1158.
16. Lei, C., Qian, K., Li, T., Zhang, S., Fu, W., Ding, M., and Hu, S. (2020). Neutralization of SARS-CoV-2 spike pseudotyped virus by recombinant ACE2-Ig. *Nat. Commun.* *11*, 2070.
17. Liu, P., Wysocki, J., Souma, T., Ye, M., Ramirez, V., Zhou, B., Wilsbacher, L.D., Quaggin, S.E., Battle, D., and Jin, J. (2018). Novel ACE2-Fc chimeric fusion provides long-lasting hypertension control and organ protection in mouse models of systemic renin angiotensin system activation. *Kidney Int.* *94*, 114–125.
18. Linsky, T.W., Vergara, R., Codina, N., Nelson, J.W., Walker, M.J., Su, W., Hsiang, T.Y., Esser-Nobis, K., Yu, K., Hou, Y.J., et al. (2020). De novo design of ACE2 protein decoys to neutralize SARS-CoV-2. *bioRxiv*.
19. Glasgow, A., Glasgow, J., Limonta, D., Solomon, P., Lui, I., Zhang, Y., Nix, M.A., Rettko, N.J., Zha, S., Yamin, R., et al. (2020). Engineered ACE2 receptor traps potentially neutralize SARS-CoV-2. *Proc. Natl. Acad. Sci. USA* *117*, 28046–28055.
20. Chan, K.K., Dorosky, D., Sharma, P., Abbasi, S.A., Dye, J.M., Kranz, D.M., Herbert, A.S., and Procko, E. (2020). Engineering human ACE2 to optimize binding to the spike protein of SARS coronavirus 2. *Science* *369*, 1261–1265.
21. Liu, P., Xie, X., Gao, L., and Jin, J. (2020). Designed variants of ACE2-Fc that decouple anti-SARS-CoV-2 activities from unwanted cardiovascular effects. *Int. J. Biol. Macromol.* *165* (Pt B), 1626–1633.
22. Linsky, T.W., Vergara, R., Codina, N., Nelson, J.W., Walker, M.J., Su, W., Barnes, C.O., Hsiang, T.Y., Esser-Nobis, K., Yu, K., et al. (2020). De novo design of potent and resilient hACE2 decoys to neutralize SARS-CoV-2. *Science* *370*, 1208–1214.
23. Payandeh, Z., Rahbar, M.R., Jahangiri, A., Hashemi, Z.S., Zakeri, A., Jafarizadeh, M., Rasaei, M.J., and Khalili, S. (2020). Design of an engineered ACE2 as a novel therapeutics against COVID-19. *J. Theor. Biol.* *505*, 110425.
24. Freitas, F.C., Ferreira, P.H.B., Favaro, D.C., and Oliveira, R.J. (2021). Shedding Light on the Inhibitory Mechanisms of SARS-CoV-1/CoV-2 Spike Proteins by ACE2-Designed Peptides. *J. Chem. Inf. Model.* *61*, 1226–1243.
25. Rodríguez-Fuentes, D.E., Fernández-Garza, L.E., Samia-Meza, J.A., Barrera-Barrera, S.A., Caplan, A.L., and Barrera-Saldaña, H.A. (2021). Mesenchymal Stem Cells Current Clinical Applications: A Systematic Review. *Arch. Med. Res.* *52*, 93–101.
26. Main, H., Munsie, M., and O'Connor, M.D. (2014). Managing the potential and pitfalls during clinical translation of emerging stem cell therapies. *Clin. Transl. Med.* *3*, 10.
27. Hass, R., Kasper, C., Böhm, S., and Jacobs, R. (2011). Different populations and sources of human mesenchymal stem cells (MSC): A comparison of adult and neonatal tissue-derived MSC. *Cell Commun. Signal.* *9*, 12.
28. Ball, L.M., Bernardo, M.E., Roelofs, H., Lankester, A., Cometa, A., Egeler, R.M., Locatelli, F., and Fibbe, W.E. (2007). Cotransplantation of ex vivo expanded mesenchymal stem cells accelerates lymphocyte recovery and may reduce the risk of graft failure in haploidentical hematopoietic stem-cell transplantation. *Blood* *110*, 2764–2767.
29. Le Blanc, K., Frasson, F., Ball, L., Locatelli, F., Roelofs, H., Lewis, I., Lanino, E., Sundberg, B., Bernardo, M.E., Remberger, M., et al.; Developmental Committee of the European Group for Blood and Marrow Transplantation (2008). Mesenchymal stem cells for treatment of steroid-resistant, severe, acute graft-versus-host disease: a phase II study. *Lancet* *371*, 1579–1586.
30. Duijvestein, M., Vos, A.C., Roelofs, H., Wildenberg, M.E., Wendrich, B.B., Verspaget, H.W., Kooy-Winkelaar, E.M., Koning, F., Zwaginga, J.J., Fidler, H.H., et al. (2010). Autologous bone marrow-derived mesenchymal stromal cell treatment for refractory luminal Crohn's disease: results of a phase I study. *Gut* *59*, 1662–1669.
31. Ranganath, S.H., Levy, O., Inamdar, M.S., and Karp, J.M. (2012). Harnessing the mesenchymal stem cell secretome for the treatment of cardiovascular disease. *Cell Stem Cell* *10*, 244–258.
32. Lythgoe, M.P., and Middleton, P. (2020). Ongoing Clinical Trials for the Management of the COVID-19 Pandemic. *Trends Pharmacol. Sci.* *41*, 363–382.
33. Hoffmann, M., Kleine-Weber, H., Schroeder, S., Krüger, N., Herrler, T., Erichsen, S., Schiergens, T.S., Herrler, G., Wu, N.H., Nitsche, A., et al. (2020). SARS-CoV-2 Cell Entry Depends on ACE2 and TMPRSS2 and Is Blocked by a Clinically Proven Protease Inhibitor. *Cell* *181*, 271–280.e8.
34. Nimmerjahn, F., and Ravetch, J.V. (2008). Fcγ receptors as regulators of immune responses. *Nat. Rev. Immunol.* *8*, 34–47.
35. Kiyoshi, M., Caaveiro, J.M., Kawai, T., Tashiro, S., Ide, T., Asaoka, Y., Hatayama, K., and Tsumoto, K. (2015). Structural basis for binding of human IgG1 to its high-affinity human receptor FcγRI. *Nat. Commun.* *6*, 6866.
36. Hamming, I., Cooper, M.E., Haagmans, B.L., Hooper, N.M., Korstanje, R., Osterhaus, A.D., Timens, W., Turner, A.J., Navis, G., and van Goor, H. (2007). The emerging role of ACE2 in physiology and disease. *J. Pathol.* *212*, 1–11.
37. Jiang, F., Yang, J., Zhang, Y., Dong, M., Wang, S., Zhang, Q., Liu, F.F., Zhang, K., and Zhang, C. (2014). Angiotensin-converting enzyme 2 and angiotensin 1-7: novel therapeutic targets. *Nat. Rev. Cardiol.* *11*, 413–426.
38. Wysocki, J., Schulze, A., and Battle, D. (2019). Novel Variants of Angiotensin Converting Enzyme-2 of Shorter Molecular Size to Target the Kidney Renin Angiotensin System. *Biomolecules* *9*, 886.
39. Yao, X., Huang, J., Zhong, H., Shen, N., Faggioni, R., Fung, M., and Yao, Y. (2014). Targeting interleukin-6 in inflammatory autoimmune diseases and cancers. *Pharmacol. Ther.* *141*, 125–139.
40. Lee, D.W., Gardner, R., Porter, D.L., Louis, C.U., Ahmed, N., Jensen, M., Grupp, S.A., and Mackall, C.L. (2014). Current concepts in the diagnosis and management of cytokine release syndrome. *Blood* *124*, 188–195.

41. Xu, X., Han, M., Li, T., Sun, W., Wang, D., Fu, B., Zhou, Y., Zheng, X., Yang, Y., Li, X., et al. (2020). Effective treatment of severe COVID-19 patients with tocilizumab. *Proc. Natl. Acad. Sci. USA* *117*, 10970–10975.
42. Toniati, P., Piva, S., Cattalini, M., Garrafa, E., Regola, F., Castelli, F., Franceschini, F., Airò, P., Bazzani, C., Beindorf, E.A., et al. (2020). Tocilizumab for the treatment of severe COVID-19 pneumonia with hyperinflammatory syndrome and acute respiratory failure: A single center study of 100 patients in Brescia, Italy. *Autoimmun. Rev.* *19*, 102568.
43. Walsh, E.E., Frenck, R.W., Jr., Falsey, A.R., Kitchin, N., Absalon, J., Gurtman, A., Lockhart, S., Neuzil, K., Mulligan, M.J., Bailey, R., et al. (2020). Safety and Immunogenicity of Two RNA-Based Covid-19 Vaccine Candidates. *N. Engl. J. Med.* *383*, 2439–2450.
44. Polack, F.P., Thomas, S.J., Kitchin, N., Absalon, J., Gurtman, A., Lockhart, S., Perez, J.L., Pérez Marc, G., Moreira, E.D., Zerbini, C., et al.; C4591001 Clinical Trial Group (2020). Safety and Efficacy of the BNT162b2 mRNA Covid-19 Vaccine. *N. Engl. J. Med.* *383*, 2603–2615.
45. Barnes, C.O., Jette, C.A., Abernathy, M.E., Dam, K.A., Esswein, S.R., Gristick, H.B., Maluyutin, A.G., Sharaf, N.G., Huey-Tubman, K.E., Lee, Y.E., et al. (2020). SARS-CoV-2 neutralizing antibody structures inform therapeutic strategies. *Nature* *588*, 682–687.
46. Chen, P., Nirula, A., Heller, B., Gottlieb, R.L., Boscia, J., Morris, J., Huhn, G., Cardona, J., Mocherla, B., Stosor, V., et al.; BLAZE-1 Investigators (2021). SARS-CoV-2 Neutralizing Antibody LY-CoV555 in Outpatients with Covid-19. *N. Engl. J. Med.* *384*, 229–237.
47. Ju, B., Zhang, Q., Ge, J., Wang, R., Sun, J., Ge, X., Yu, J., Shan, S., Zhou, B., Song, S., et al. (2020). Human neutralizing antibodies elicited by SARS-CoV-2 infection. *Nature* *584*, 115–119.
48. Mulligan, M.J., Lyke, K.E., Kitchin, N., Absalon, J., Gurtman, A., Lockhart, S., Neuzil, K., Raabe, V., Bailey, R., Swanson, K.A., et al. (2020). Phase I/II study of COVID-19 RNA vaccine BNT162b1 in adults. *Nature* *586*, 589–593.
49. Voysey, M., Clemens, S.A.C., Madhi, S.A., Weckx, L.Y., Folegatti, P.M., Aley, P.K., Angus, B., Baillie, V.L., Barnabas, S.L., Bhorat, Q.E., et al.; Oxford COVID Vaccine Trial Group (2021). Safety and efficacy of the ChAdOx1 nCoV-19 vaccine (AZD1222) against SARS-CoV-2: an interim analysis of four randomised controlled trials in Brazil, South Africa, and the UK. *Lancet* *397*, 99–111.
50. Zost, S.J., Gilchuk, P., Case, J.B., Binshtein, E., Chen, R.E., Nkolola, J.P., Schäfer, A., Reidy, J.X., Trivette, A., Nargi, R.S., et al. (2020). Potently neutralizing and protective human antibodies against SARS-CoV-2. *Nature* *584*, 443–449.
51. Li, Q., Wu, J., Nie, J., Zhang, L., Hao, H., Liu, S., Zhao, C., Zhang, Q., Liu, H., Nie, L., et al. (2020). The Impact of Mutations in SARS-CoV-2 Spike on Viral Infectivity and Antigenicity. *Cell* *182*, 1284–1294.e9.
52. Ozono, S., Zhang, Y., Ode, H., Sano, K., Tan, T.S., Imai, K., Miyoshi, K., Kishigami, S., Ueno, T., Iwatani, Y., et al. (2021). SARS-CoV-2 D614G spike mutation increases entry efficiency with enhanced ACE2-binding affinity. *Nat. Commun.* *12*, 848.
53. Li, W., Schäfer, A., Kulkarni, S.S., Liu, X., Martinez, D.R., Chen, C., Sun, Z., Leist, S.R., Drelich, A., Zhang, L., et al. (2020). High Potency of a Bivalent Human V_H Domain in SARS-CoV-2 Animal Models. *Cell* *183*, 429–441.e16.
54. Wu, K., Peng, G., Wilken, M., Geraghty, R.J., and Li, F. (2012). Mechanisms of host receptor adaptation by severe acute respiratory syndrome coronavirus. *J. Biol. Chem.* *287*, 8904–8911.
55. Castilho, A., Schwestka, J., Kienzl, N.F., Vavra, U., Grünwald-Gruber, C., Izadi, S., Hiremath, C., Niederhöfer, J., Laurent, E., Monteil, V., et al. (2021). Generation of enzymatically competent SARS-CoV-2 decoy receptor ACE2-Fc in glycoengineered *Nicotiana benthamiana*. *Biotechnol. J.* Published online January 22, 2021. <https://doi.org/10.1002/biot.202000566>.
56. Han, Y., and Král, P. (2020). Computational Design of ACE2-Based Peptide Inhibitors of SARS-CoV-2. *ACS Nano* *14*, 5143–5147.
57. Morse, J.S., Lalonde, T., Xu, S., and Liu, W.R. (2020). Learning from the Past: Possible Urgent Prevention and Treatment Options for Severe Acute Respiratory Infections Caused by 2019-nCoV. *ChemBioChem* *21*, 730–738.
58. Qi, X., Li, F., Wu, Y., Cheng, C., Han, P., Wang, J., and Yang, X. (2019). Optimization of 4-1BB antibody for cancer immunotherapy by balancing agonistic strength with FcγR affinity. *Nat. Commun.* *10*, 2141.
59. Hogarth, P.M., and Pietersz, G.A. (2012). Fc receptor-targeted therapies for the treatment of inflammation, cancer and beyond. *Nat. Rev. Drug Discov.* *11*, 311–331.
60. Frenette, P.S., Pinho, S., Lucas, D., and Scheiermann, C. (2013). Mesenchymal stem cell: keystone of the hematopoietic stem cell niche and a stepping-stone for regenerative medicine. *Annu. Rev. Immunol.* *31*, 285–316.
61. von Bahr, L., Batsis, I., Moll, G., Hägg, M., Szakos, A., Sundberg, B., Uzunel, M., Ringden, O., and Le Blanc, K. (2012). Analysis of tissues following mesenchymal stromal cell therapy in humans indicates limited long-term engraftment and no ectopic tissue formation. *Stem Cells* *30*, 1575–1578.
62. Caplan, H., Olson, S.D., Kumar, A., George, M., Prabhakara, K.S., Wenzel, P., Bedi, S., Toledano-Furman, N.E., Triolo, F., Kamhieh-Milz, J., et al. (2019). Mesenchymal Stromal Cell Therapeutic Delivery: Translational Challenges to Clinical Application. *Front. Immunol.* *10*, 1645.
63. Moll, G., Hoogduijn, M.J., and Ankrum, J.A. (2020). Editorial: Safety, Efficacy and Mechanisms of Action of Mesenchymal Stem Cell Therapies. *Front. Immunol.* *11*, 243.
64. Moll, G., Drzeniek, N., Kamhieh-Milz, J., Geissler, S., Volk, H.D., and Reinke, P. (2020). MSC Therapies for COVID-19: Importance of Patient Coagulopathy, Thromboprophylaxis, Cell Product Quality and Mode of Delivery for Treatment Safety and Efficacy. *Front. Immunol.* *11*, 1091.
65. Moll, G., Ankrum, J.A., Kamhieh-Milz, J., Bieback, K., Ringden, O., Volk, H.D., Geissler, S., and Reinke, P. (2019). Intravascular Mesenchymal Stromal/Stem Cell Therapy Product Diversification: Time for New Clinical Guidelines. *Trends Mol. Med.* *25*, 149–163.
66. Wu, Z., Zhang, S., Zhou, L., Cai, J., Tan, J., Gao, X., Zeng, Z., and Li, D. (2017). Thromboembolism Induced by Umbilical Cord Mesenchymal Stem Cell Infusion: A Report of Two Cases and Literature Review. *Transplant. Proc.* *49*, 1656–1658.